

## Depth-dependent spectroscopic defect characterization of the interface between plasma-deposited SiO<sub>2</sub> and silicon

J. Schäfer,<sup>a)</sup> A. P. Young,<sup>b)</sup> and L. J. Brillson<sup>c)</sup>

*Center for Materials Research, Department of Physics, Ohio State University, Columbus, Ohio 43210*

H. Niimi and G. Lucovsky

*Department of Physics, North Carolina State University, Raleigh, North Carolina 27695*

(Received 5 May 1998; accepted for publication 8 June 1998)

We demonstrate the use of low-energy cathodoluminescence spectroscopy (CLS) to study optical transitions at defect bonding arrangements at Si–SiO<sub>2</sub> interfaces prepared by low-temperature plasma deposition. Variable-depth excitation achieved by different electron injection energies provides a clear distinction between luminescence derived from (i) the near-interface region of the oxide film, (ii) the Si–SiO<sub>2</sub> interface, and (iii) the underlying crystalline Si substrate. Cathodoluminescence bands at ~0.8 and 1 eV are assigned to interfacial Si atom dangling bonds with different numbers of back-bonded Si and O atoms. CLS also reveals higher photon energy features: two bands at ~1.9 and 2.7 eV assigned to suboxide bonding defects in the as-grown oxide films, as well as a substrate-related feature at ~3.4 eV. The effects of hydrogenation at 400 °C and rapid thermal annealing at 900 °C, and especially the combination of both process steps is shown to dramatically reduce the intensities of the CLS features assigned to interfacial and suboxide bonding defects. © 1998 American Institute of Physics. [S0003-6951(98)03632-8]

As device dimensions are scaled into the deep submicron to achieve higher levels of integration, there must be corresponding decreases in the oxide-equivalent thickness of dielectrics,  $t_{\text{ox,eq}}$ . For example, channel lengths in field effect transistor (FET) devices are projected to decrease to ~50 nm by the year 2012, at which time  $t_{\text{ox,eq}}$  values will be at most 1 nm.<sup>1</sup> At these thicknesses, tunneling is the dominant transport mechanism for leakage current, and defects at the Si–SiO<sub>2</sub> interface will limit device performance and reliability.<sup>2</sup> In addition, the necessity to produce Si–SiO<sub>2</sub> interfaces with selective incorporation of nitrogen, and ultra-thin SiO<sub>2</sub> layers that form a substrate for high- $K$  dielectrics such as TiO<sub>2</sub> or Ta<sub>2</sub>O<sub>5</sub> will mandate increased understanding and control of the chemical bonding and defect states in the immediate vicinity of the underlying Si–SiO<sub>2</sub> interface. Implicit in the development of composite gate dielectrics for FETs is the necessity to combine interface formation by thermal or plasma-assisted oxidation with either physical, chemical vapor, or plasma-assisted deposition processes. Studies performed to date on Si–SiO<sub>2</sub> interfaces, and nitrided Si–SiO<sub>2</sub> interfaces, have demonstrated that transitions regions with suboxide bonding are created during thermal or plasma-assisted oxidation, and that the extent of these regions is decreased significantly after a 900 °C anneal.<sup>3</sup>

In this letter, we report on studies of Si–SiO<sub>2</sub> structures by low-energy cathodoluminescence spectroscopy (CLS).<sup>4</sup> For these heterostructures with 5-nm-thick oxides, the Si–SiO<sub>2</sub> interface was formed by 300 °C remote plasma-assisted oxidation (RPAO), and the remainder of the SiO<sub>2</sub> component of the heterostructure was formed by 300 °C remote plasma enhanced chemical vapor deposition

(RPECVD).<sup>5,6</sup> The work includes studies of films subjected to postdeposition annealing and hydrogenation.

The films were prepared on ~10 Ω cm boron-doped *p*-Si(100) substrates, cleaned by repeated oxidation and etch-back in hydrofluoric acid, with a final oxide-removal etch in 1 at. % HF. The Si–SiO<sub>2</sub> structures were formed by a two-step plasma process:<sup>5</sup> (i) RPAO to form the interface and grow ~0.5–0.6 nm of SiO<sub>2</sub>; and (ii) RPECVD to deposit the bulk oxide film, for a total SiO<sub>2</sub> thickness of ~5 nm. For each step, the substrate temperature was 300 °C, the process pressure 0.3 Torr, and the plasma power 30 W. The active species for the RPAO were extracted from a remote He/O<sub>2</sub> (10:1) plasma. For the film deposition, silane diluted in He (2%) was delivered downstream, and a He/O<sub>2</sub> mixture was excited in the plasma tube He/O<sub>2</sub>/SiH<sub>4</sub>=200/20/0.2. For annealing studies, samples were subjected to either a 400 °C anneal in forming gas (N<sub>2</sub>/H<sub>2</sub>) for 30 min, a rapid thermal anneal (RTA) at 900 °C in Ar for 30 s, or both the RTA and then the 400 °C N<sub>2</sub>/H<sub>2</sub> anneal. The specimens were transferred in air into an ultrahigh vacuum (UHV) chamber for analysis. Auger electron spectra indicated submonolayer carbon contamination which was easily removed by an anneal at 300 °C. CLS studies were carried out at room temperature with electron beam energies between 0.6 and 4.5 keV and beam currents of 1–4 μA on a spot ~100 μm in diameter. Even after exposure to an electron beam fluence an order of magnitude higher than used for obtaining the spectra, there was no observable spectroscopic or visual *e*-beam damage. The luminescence was recorded with a monochromator set to ~50 meV resolution using a Ge detector for the infrared, and a S-20 photocathode for the visible-to-ultraviolet spectral range. The spectra contain no correction for the optical system response since this was known to vary slowly at the relevant energy ranges.

<sup>a)</sup>Electronic mail: schaefer@ee.eng.ohio-state.edu

<sup>b)</sup>Also with Department of Electrical Engineering.

<sup>c)</sup>Also with the Department of Electrical Engineering.

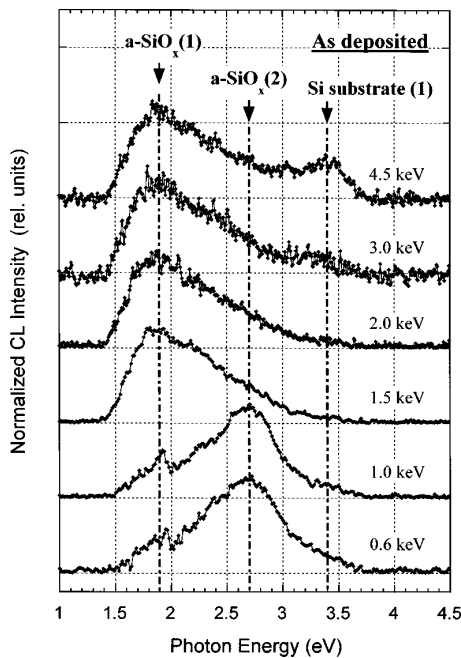


FIG. 1. CL spectra of the as-deposited ultrathin silicon dioxide with a S-20 photodetector for varying incident electron beam energy. Close to the film surface (low excitation energies), defects characteristic of substoichiometric  $\text{SiO}_2$  are detected at 2.7 eV, while near the interface (intermediate excitation energies) such  $\alpha\text{-SiO}_x$  bonding environments show defect luminescence at 1.9 eV. Evidence for direct transitions involving the Si substrate appears at high beam energies.

CLS spectra of the as-prepared plasma-deposited 50 Å film appear in Fig. 1 as a function of electron energy, and therefore surface penetration depth. For 1.0 keV one estimates a depth of maximum energy loss due to electron-hole pair creation of about 30 Å, which is known to vary with beam energy  $E$  as  $\sim E^{1.7}$ .<sup>7</sup> The spectra were taken with constant excitation power and thereby a nearly constant electron-hole pair generation rate. Since other effects such as spatial changes in the electronic density of states may also influence the intensity, the displayed data are normalized to the same peak height. The spectra were taken with the S-20 phototube which is most sensitive above 1.4 eV. For intermediate beam energies, defined here as 1.5 and 2.0 keV, a prominent feature is observed at 1.9 eV. For lower beam energies, 0.6 and 1.0 keV, the 1.9 eV feature decreases in intensity, and a new defect feature emerges at about 2.7 eV. At higher energies, 3.0 and 4.5 keV, (i) the 1.9 eV peak remains, (ii) the 2.7 eV peak is not observed, and (iii) there is an additional spectral peak at 3.4 eV that is most readily observed as a distinct feature for the 4.5 keV excitation.

In the infrared spectral range recorded with the Ge detector and shown in Fig. 2, two luminescence features were detected at  $\sim 0.8$  eV and at 1.0 eV over the entire range of excitation energies. The relative intensity of 1.0 eV peak increases with increasing excitation energy, indicating that it is a component associated with the bulk Si as well as a component associated with the interfacial layer.

The effect of postdeposition annealing under different ambients has also been measured and spectra obtained with the S-20 phototube and Ge detector are presented in Fig. 3. The top two traces in Fig. 3 indicate the effects of the 400 °C forming gas anneal. These spectra, taken at an excitation

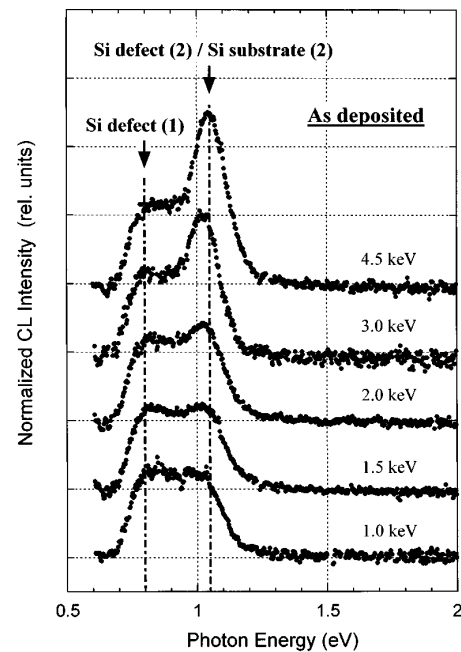


FIG. 2. CL spectra of the as-deposited silicon dioxide film, in the infrared regime using a Ge detector. Silicon defect emission is evident at 0.8 eV. The spectra are normalized to this peak. Band edge luminescence from the crystalline substrate increases with increasing excitation voltage and hence increasing excitation depth.

energy of 2.0 keV reveal only small changes in the relative intensities of the 0.8 and 1 eV bands, but a pronounced decrease in the broad band at 1.9 eV after the anneal. Additionally, the intensity remains relatively unchanged for the 3.4 eV transition after the anneal. Rapid thermal annealing (RTA) in argon gas at 900 °C at ambient pressure caused the broad band at 1.9 eV to vanish below the level of detection. The 900 °C anneal enhances the 3.4 eV feature, but does not change the relative intensity of the 0.8 and 1 eV bands. Figure 3 also shows that the features at 0.8 and  $\sim 1$  eV change significantly after being subjected to an RTA at 900 °C followed by hydrogenation at 400 °C. Relative to the 900 °C anneal spectra, the intensities at 0.8 and  $\sim 1$  eV decrease dramatically, and the spectral intensity of the 3.4 eV band also decreases.

The CLS studies have identified five distinct spectral features at 0.8,  $\sim 1$ , 1.9, 2.7, and 3.4 eV. At first sight it might be tempting to try to interpret these features in terms of defect luminescence bands previously identified in irradiated quartz,<sup>8</sup> silica glass,<sup>9</sup> and thermally grown silicon dioxide,<sup>10,11</sup> as well as oxidized porous silicon.<sup>12</sup> However, since the most dramatic changes in the CLS spectra occur after the combined 900 °C RTA and 400 °C rehydrogenation, it is more instructive to compare these results with annealing studies on similarly prepared Si-SiO<sub>2</sub> interfaces that have relied on optical and electrical characterization.<sup>3,13</sup> Summarizing the results in Refs. 3 and 13, and references therein: (i) as grown oxides, whether by thermal, chemical, or plasma-assisted techniques, display significant suboxide bonding in a transition region at least 0.5 nm thick between the Si substrate and the SiO<sub>2</sub> film, (ii) postdeposition anneals in an inert ambient at a temperatures of approximately 900 °C for at least 30 s reduces these suboxide regions sig-

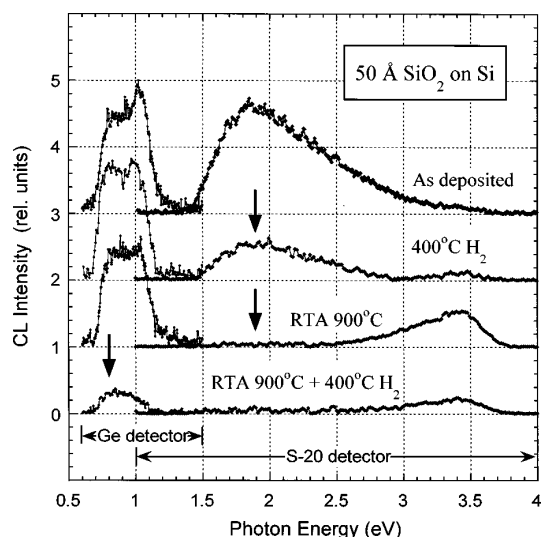


FIG. 3. Evolution of defect bands versus annealing treatments, for the same 2.0 keV excitation energy. Spectral intensities between the two detectors are not normalized, but for each detector the relative intensities of the series of samples directly reflect the luminescence efficiency. A dramatic decrease in defect density is observed at 1.9 eV upon annealing at 900 °C. Posthydrogenation at 400 °C induces an additional decrease at 0.8 eV.

nificantly, as seen by Auger electron spectroscopy, x-ray photoelectron spectroscopy, and optical second harmonic generation (SHG). An electron transmission interference technique<sup>14</sup> shows that growth of an oxide at 900 °C is not equivalent with respect to transition region reduction, to growth at 900 °C followed by annealing at 900 °C. In addition, postoxidation annealing at 900 °C of interfaces prepared by both plasma and thermal oxidation improves electrical performance, reducing interface state densities down to at least the mid  $10^{10} \text{ cm}^{-2} \text{ eV}^{-1}$  range, and improving resistance to hot carrier stressing in field effect transistors.<sup>15</sup> Finally, as discussed in Refs. 3 and 13, the effects of interface nitridation at the monolayer level, both on optical properties such as SHG, and improved electrical performance are only evident after a 900 °C anneal, presumably due to reduction of suboxide transition regions.

Based on the energy dependence of the CLS as shown in Figs. 1 and 2, as well as the annealing results of Fig. 3 the following assignments are made. The 0.8 eV feature and the 1 eV feature are related to interfacial Si-atom dangling bond defects with different numbers of Si and O atoms back bonded to the Si atom with the dangling bond. These assignments are based on the photon energy of the luminescence,<sup>16,17</sup> and are consistent with the changes in the concentration of these defects after a prolonged vacuum anneal. A vacuum anneal by itself will remove H atoms from the dangling bonds, increasing CLS yield;<sup>18</sup> however, following an anneal in a H-containing ambient the dangling bond density of states is reduced by H-atom attachment.<sup>19</sup> Model calculations<sup>17</sup> and experimental results on defects in intentionally oxygenated *a*-Si:H<sup>20</sup> suggest that the 0.8 eV dangling bond is associated with a Si atom that has three Si-nearest neighbors, whereas for the 1 eV defect the Si atom with the dangling bond has two Si- and one O-nearest neighbors. As seen in Fig. 2, for the higher electron beam energies the 1 eV band may also contain an additional substrate con-

tribution; e.g., from disorder-induced near-band edge luminescence.

The features at 1.9 and 2.7 eV are assigned to luminescent transitions involving an as yet unspecified suboxide bonding defect in the transition region *near* the grown interface. Based on the electron energy dependence, the 1.9 eV feature is located closer to the interface than the 2.7 eV feature. Since both of these bands are removed completely after 900 °C annealing, the assignments are consistent with significant suboxide reductions found by other characterization methods.<sup>3,13</sup> Finally, the 3.4 eV peak likely contains contributions from a substrate bulk resonance associated with the lowest direct band gap in crystalline Si. The CLS peak is at essentially the same energy as the sharp feature in the imaginary part of the dielectric constant,  $\epsilon_2$ , which is due to optical transitions in the Brillouin zone between  $\Gamma$  and *L* along the  $\Lambda$  direction.<sup>21</sup>

In summary, the CLS study has provided depth-resolved information relative to interfacial transition regions and interface bonding defects which complement the results of other studies. In particular, this information is important in helping identify local bonding environments which contribute to electronically active defects at Si-SiO<sub>2</sub> interfaces. Therefore, such direct detection of deep electronic defect levels can help guide further development of low defect semiconductor-dielectric interfaces.

This work is supported in part by NSF Grant No. DMR 9711851 at the Ohio State University, and by ONR, SRC, and the NSF Engineering Research Center at North Carolina State University.

<sup>1</sup>The National Technology Roadmap for Semiconductors, Semiconductor Industry Association (SEMATECH, Austin, TX, 1997).

<sup>2</sup>D. A. Buchanan and S.-H. Lo, in *The Physics and Chemistry of SiO<sub>2</sub> and the Si-SiO<sub>2</sub> Interface*, edited by H. Z. Massoud, E. H. Poindexter, and C. R. Helms (Electrochemical Society, Pennington, NJ, 1996), pp. 319-322.

<sup>3</sup>G. Lucovsky, A. Banerjee, B. Hinds, B. Claffin, K. Kon, and H. Yang, *J. Vac. Sci. Technol.* **15**, 1074 (1997).

<sup>4</sup>L. J. Brillson, H. W. Richter, M. L. Slade, B. A. Weinstein, and Y. Shapira, *J. Vac. Sci. Technol. A* **3**, 1011 (1985).

<sup>5</sup>T. Yasuda, Y. Ma, S. Habermehl, and G. Lucovsky, *Appl. Phys. Lett.* **60**, 434 (1992).

<sup>6</sup>S. V. Hattangady, R. G. Alley, G. G. Fountain, R. J. Markunas, G. Lucovsky, and D. Temple, *J. Appl. Phys.* **73**, 7635 (1993).

<sup>7</sup>L. J. Brillson and R. E. Viturro, *Scanning Microsc.* **2**, 789 (1988).

<sup>8</sup>M. A. S. Kalceff and M. R. Phillips, *Phys. Rev. B* **52**, 3122 (1995).

<sup>9</sup>R. Tohmon, Y. Shimogaichi, H. Mizuno, Y. Ohki, K. Nagasawa, and Y. Hama, *Phys. Rev. Lett.* **62**, 1388 (1989).

<sup>10</sup>H. Koyama, *J. Appl. Phys.* **51**, 2228 (1980).

<sup>11</sup>L. N. Skuja and W. Entzian, *Phys. Status Solidi A* **96**, 191 (1986).

<sup>12</sup>F. Koch and V. Petrova-Koch, *J. Non-Cryst. Solids* **198-200**, 840 (1996).

<sup>13</sup>G. Lucovsky, H. Niimi, K. Koh, D. R. Lee, and Z. Jing, in Ref. 2, p. 441.

<sup>14</sup>X. Chen and J. M. Gibson, *Appl. Phys. Lett.* **70**, 1462 (1997).

<sup>15</sup>D. R. Lee, C. Parker, J. R. Hauser, and G. Lucovsky, *J. Vac. Sci. Technol. B* **13**, 1788 (1995).

<sup>16</sup>R. A. Street, *Adv. Phys.* **30**, 593 (1981).

<sup>17</sup>G. Lucovsky and S. Y. Lin, in *Optical Effects in Semiconductors*, AIP Conf. Proc. 120, edited by P. C. Taylor and S. G. Bishop (AIP, New York, 1984), p. 55.

<sup>18</sup>A. P. Young, J. Schäfer, G. Jessen, R. Bandhu, L. J. Brillson, H. Niimi, and G. Lucovsky, *J. Vac. Sci. Technol.* (in press).

<sup>19</sup>G. Lucovsky, Z. Jing, and D. R. Lee, *J. Vac. Sci. Technol. B* **14**, 2832 (1996).

<sup>20</sup>C. E. Mikkelsen and J. D. Cohen, *Phys. Rev. B* **41**, 1529 (1990).

<sup>21</sup>D. E. Aspnes and A. A. Studna, *Phys. Rev. B* **27**, 985 (1983).